The Nature of Spectral Transitions in Accreting Black Holes: The Case of Cyg X-1

Juri Poutanen[1,2]⋆, Julian H. Krolik[3]⋆, and Felix Ryde[2]⋆

[1] *Uppsala Observatory, Box 515, S-751 20 Uppsala, Sweden; juri@astro.uu.se*
[2] *Stockholm Observatory, S-133 36 Saltsjöbaden, Sweden*
[3] *Johns Hopkins University, Baltimore, MD 21218, USA*

ABSTRACT
Accreting black holes radiate in one of several spectral states, switching from one to another for reasons that are as yet not understood. Using the best studied example, Cyg X-1, we identify the geometry and physical conditions characterizing these states. In particular, we show that in the hard state most of the accretion energy is dissipated in a corona-like structure which fills the inner few tens of gravitational radii around the black hole and has Compton optical depth of order unity. In this state, an optically thick accretion disc extends out to greater distance, but penetrates only a short way into the coronal region. In the soft state, the optically thick disc moves inward and receives the majority of the dissipated energy, while the "corona" becomes optically thin and extends around much of the inner disc. The mass accretion rate in both states is $\sim 1 \times 10^{-8} M_\odot$ yr^{-1}.

Key words: accretion, accretion discs – gamma-rays: theory – radiation mechanisms: non-thermal – stars: individual (Cygnus X-1) – X-ray: general – X-ray: stars

1 SPECTRAL STATES OF GBHC

For many years we have known that Galactic Black Hole Candidates (GBHC) radiate X-rays in one of several spectral states, switching suddenly from one to another. Although intermediate states are sometimes also seen, the spectral states of GBHCs are best typified by their extremes: a "hard" state (sometimes also called the "low" state because the $2 - 10$ keV flux is relatively weak in this state), and a "soft" state (sometimes also called the "high" state because the $2 - 10$ keV flux is relatively strong). The spectrum in both states may be roughly described as the sum of two components: a blackbody, and a power-law with an exponential cut-off. In the soft state the blackbody is relatively prominent and the power-law is steep; in the hard state more energy is carried in the power-law, whose slope is then shallower.

More specifically, in the soft state (SS), the $0.1 - 5$ keV band is dominated by a component best described as either a blackbody with temperature $0.3 - 1$ keV, or perhaps a sum of blackbodies all with temperatures in that range (Mitsuda et al. 1984). The slope (in energy units) of the power-law between 5 and 40 keV is generally $1.0 - 1.5$ (Tanaka & Lewin 1995). OSSE and RXTE data, when fitted with a model consisting of a power-law with an exponential cut-off, show

slopes between 1.6 and 2.1 and a cut-off energy (although not very well determined) $\gtrsim 200$ keV (Grove et al. 1997, see also Phlips et al.1996, Cui et al. 1996 and Gierliński et al. 1997b for observations of Cyg X-1). Most of the energy is emitted in the soft thermal component.

In the hard state (HS), the soft component is much less luminous, and can be represented by a black body with a temperature 0.1-0.2 keV (Bałucińska-Church et al. 1995; Ebisawa et al. 1996). Most of the energy is emitted in the hard tail, which can be represented by a power-law of slope $0.3 - 0.7$ with an exponential cut-off at about 100 keV (Tanaka & Lewin 1995; Phlips et al. 1996; Grove et al. 1997; Gierliński et al. 1997a; Zdziarski et al. 1997). The *Ginga* spectrum of Cyg X-1 also shows a clear sign of hardening at about 10 keV accompanied by a fluorescent Fe Kα line at $\sim$ 6.4 keV. These effects are most easily interpreted as the signature of Compton reflection from cold matter in the vicinity of the hard X/γ-ray source. In this interpretation, the strength of the Fe Kα line and the reflection bump requires the cold matter to subtend a solid angle $\Omega/2\pi \approx 0.4$ around the hard X-ray source (Ebisawa et al. 1996; Gierliński et al. 1997a).

It was originally thought that these systems were much more luminous in the soft state than in the hard. However, in a striking new result, Zhang et al. (1997b) have shown that the *bolometric* luminosity of Cyg X-1 changes only slightly despite dramatic changes in spectral shape. In view of this,

⋆ E-mail: juri@astro.uu.se (JP); jhk@gauss.pha.jhu.edu (JHK); felix@astro.su.se (FR)

we eschew the designations "high" and "low", and strongly urge that in the future these states be called "soft" and "hard".

What exactly is happening in these sources when they switch spectral state has long been a puzzle. However, in recent years advances have been made both on the observational side (most importantly, hard X-ray/soft γ-ray observations now give us a clearer picture of that portion of the spectrum) and on the theoretical side (we now understand much better how thermal Comptonization works when the seed photons are produced in large part by reprocessing part of the hard X-ray output). Making use of this progress, we can now use the observed character of the spectrum in these states to determine the geometry and energy dissipation distribution in an accreting black hole system in *all* its different spectral states. The geometry and energy dissipation distribution inferred purely on the basis of *radiation* physics can then be used to guide efforts to obtain *dynamical* explanations for the changes in spectral state. Because the observational data are best for Cyg X-1, we illustrate our method here by applying it to that source. As will be seen, even in this example, there are still uncertainties which prevent some of our conclusions from being as strong as might be possible in principle, but the bulk of this program is now realizable in the case of Cyg X-1, and it may soon be possible to extend it to other sources.

2   DIRECTLY MEASURED PARAMETERS AND INFERENCES FROM ANALYTIC ARGUMENTS

We attribute the two components with which the spectra are fit to two physically distinct, but related, regions: an optically thick, quasi-thermal region which is responsible for the blackbody component (the accretion disc?); and an optically thin very hot region which radiates the hard X-rays (a corona?). We call the intrinsic dissipation rates in the "disc" and "corona" $L_s^{\rm intr}$ and L_h, respectively. The scale over which the "disc" radiates most of its energy is R_s.

Following the consensus in the field (Shapiro, Lightman & Eardley 1976; Haardt, Maraschi & Ghisellini 1994; Stern et al. 1995; Zdziarski et al. 1997), we suppose that the hard X-rays are produced by thermal Comptonization. The seed photons for this process are partly created locally (by thermal bremsstrahlung or synchro-cyclotron radiation: Narayan & Yi 1995) and are partly created in the quasi-thermal region. The luminosity of the quasi-thermal region is in turn partly due to local energy dissipation, and partly due to reradiation of hard X-rays created in the "corona".

In this model, the shape of the Comptonized spectrum produced by the "corona" may be quite adequately described phenomenologically by two parameters: the power-law slope α, the exponential cut-off energy E_c. Two more parameters (the effective temperature T_s and $L_s^{\rm obs}$) define the soft part of the radiation. The ratio of the observed hard luminosity to the observed soft luminosity, $L_h^{\rm obs}/L_s^{\rm obs}$, and the magnitude of the reflection bump $C \equiv \Omega/2\pi$ ($C = 1$ corresponds to the amplitude of reflection expected from a slab subtending a 2π solid angle around an isotropic X-ray source atop the slab) complete the set of observables. These phenomenological parameters are determined by two dimen-

Table 1. Observational characteristics of Cyg X-1 in its soft and hard states

Parameter	Hard state	Soft state
$L_s^{\rm obs}$ [a]	1×10^{37} erg/s[1,2,3]	4×10^{37} erg/s[4,5]
$L_h^{\rm obs}$ [b]	4×10^{37} erg/s [4,6]	1×10^{37} erg/s [4,5]
α [c]	0.6[6]	1.6[7,9,12]
T_s [d]	0.13 keV[1,2,3]	0.4 keV[7,8,9]
E_c [e]	150 keV[6,10,11]	$\gtrsim$ 200 keV[7,10]
C [f]	0.4[3,6]	0.55[12]

[a]Observed soft luminosity (total luminosity below $\sim$ 1 keV in the HS and below $\sim$ 3 keV in the SS)
[b]Observed hard luminosity
[c]Energy spectral index
[d]Temperature of the soft component
[e]Cut-off energy of hard component
[f]Covering factor of the cold matter

References are:(1) Bałucińska & Hasinger 1991; (2) Bałucińska-Church et al. 1995; (3) Ebisawa et al. 1996; (4) Tanaka & Lewin 1995; (5) Zhang et al. 1997b; (6) Gierliński et al. 1997a; (7) Cui et al. 1996; (8) Belloni et al. 1996; (9) Dotani et al. 1996; (10) Phlips et al. 1996; (11) Zdziarski et al. 1997; (12) Gierliński et al. 1997b

sional quantities, the total dissipation rate and R_s, and four dimensionless physical parameters: the ratio $L_s^{\rm intr}/L_h$; the Compton optical depth of the "corona" τ_T; the fraction D of the light emitted by the thermal region which passes through the "corona"; and the ratio S of intrinsic seed photon production in the "corona" to the seed photon luminosity injected from outside. Another dimensionless parameter, the compactness $l_h \equiv L_h \sigma_T/(m_e c^3 R_h)$, may be used to determine the relative importance of $e^\pm$ pairs in the corona (R_h is the size of the corona). In this context it is also useful to distinguish the net lepton Compton optical depth τ_p from the total Compton optical depth (including pairs), τ_T.

We will show how all these parameters, as well as several others of physical interest, may be inferred from observable quantities. The observables on which we base this analysis for Cyg X-1 are shown in Table 1. Because Cyg X-1 varies, the numbers seen at any particular time may be somewhat different from the "typical" values we cite.

Certain of these figures deserve special comment. $L_s^{\rm obs}$ in the hard state is particularly uncertain. In works of Bałucińska-Church et al. (1995) and Ebisawa et al. (1996), the spectrum in the *ROSAT* band is fit by a sum of a blackbody and a power-law. They take $L_s^{\rm obs}$ to be only the part due to the blackbody; we believe that it is better described by the total of the two, and therefore find a soft luminosity two times greater than they do. In the soft state, C is very difficult to determine, since the amount of reflection depends on the assumed run of ionisation with radius (Chris Done, private communications). We will point out the degree to which our conclusions are sensitive to this uncertainty.

Some of the physical parameters of the system may be derived (or at least constrained) almost directly from observables. For example, the electron temperature in the corona (measured in electron rest mass units) is very closely related to the cut-off energy of the hard component: $\Theta \simeq f_x E_c/(m_e c^2)$, where f_x is a number slightly less than unity, whose exact value depends on τ_T. Similarly, $L_h \approx L_h^{\rm obs} (1 + C4\pi da/d\Omega)/(1 + C)$, where $da/d\Omega$ is the albedo per unit solid angle for Compton reflection, and we
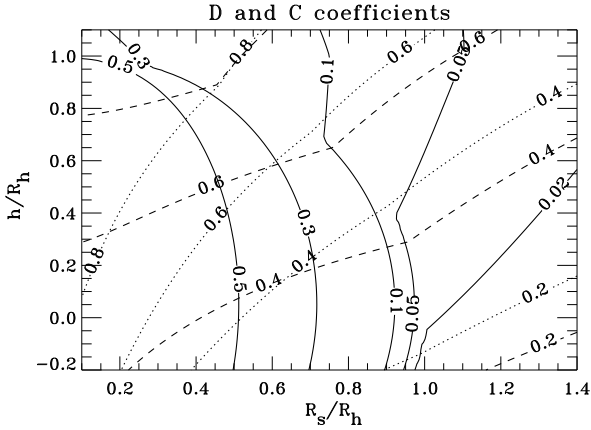
Figure 1. Coefficients D and C as function of h/R_h and R_s/R_h. Solid curves represent contours of the constant D. Dashed curves give contours of constant C for $\tau_T = 1.3$ (corresponding to the HS). Dotted curves give C for $\tau_T = 0.3$ corresponding to the SS.

Table 2. Inferred properties of Cyg X-1 in its soft and hard states

Parameter	Hard state	Soft state
Θ[a]	~ 0.2	$\gtrsim 0.3$
$L_s^{\rm intr}/L_h$[b]	$\lesssim 0.1$	~ 3
R_s[c]	500 km	100 km
$D(1+S)$[d]	0.08	0.3
τ_T[e]	$\simeq 1.3$	$\lesssim 0.35$
R_s/R_h[f]	$\simeq 0.9$	$\simeq 0.65$
h/R_h[g]	$\simeq 0.2$	$\simeq 0.5$
l_h[h]	$\simeq 20$	$\simeq 15$

[a]Electron temperature, $\Theta \equiv kT_e/mc^2$
[b]Ratio of intrinsic soft luminosity to the intrinsic hard luminosity (all the correction factors are here assumed to combine to unity)
[c]Inner radius of the cold disc
[d]Covering fraction of "corona" around thermal disc times the seed photon correction factor
[e]Radial Thomson optical depth of the hot cloud
[f]Inner radius of the disc relative to the hot cloud
[g]Elevation of the corona above to the disc relative to the size of the hot cloud
[h]Hard compactness, $l_h \equiv L_h/R_h(\sigma_T/m_e c^3)$

assumed that the hard component has an isotropic angular distribution and $\tau_T \ll 1$.

The intrinsic disc luminosity is

$$L_s^{\rm intr} = L_s^{\rm tot} - \frac{CL_h}{1+C}\left[1 - \int d\Omega\, da/d\Omega\right], \qquad (1)$$

where $L_s^{\rm tot} = L_s^{\rm obs}/p(\theta)\left[1 - D\left(1 - e^{-\tau_T}\right)\right]$ is the total soft luminosity, and $p(\theta)$ gives the angular distribution of the disc radiation (normalized so that $\int d\Omega\, p(\theta) = 4\pi$). Taking the disc emission to be approximately black body, its inner radius is

$$R_s = \left(\frac{L_s^{\rm tot}}{4\pi\sigma T_s^4}\right)^{1/2}\left(\frac{f_{\rm col}^2 f_{\rm GR}^2}{f_m}\right), \qquad (2)$$

where T_s is the effective temperature at the inner edge. The additional correction factors are: $f_{\rm col}$, the ratio between the local color temperature and the local effective temperature; $f_{\rm GR}$, which incorporates the general relativistic corrections linking the local color temperature to the observed one; and f_m, which accounts for a proper integration over the disc's surface brightness distribution. For estimates of the correction factors see, e.g., Shimura & Takahara (1995) and Zhang et al. (1997a). The combination of all these correction factors is likely to be close to unity, but is uncertain at the 50% to factor of 2 level.

We next employ the two following analytic scaling approximations for thermal Comptonization spectra found by Pietrini & Krolik (1995): $D(1+S) = 0.15\alpha^4 L_h/L_s^{\rm tot}$ and $\tau_T = 0.16/(\alpha\Theta)$. The first expresses how the power-law hardens as the heating rate in the corona increases relative to the seed photon luminosity; the second expresses the trade-off in cooling power between increasing optical depth and increasing temperature.

Finally, we assume a description of the geometry involving the minimum number of free parameters consistent with describing a reasonable universe of possibilities. We take the disc to be an annulus of inner radius R_s extending to infinite radius, with infinitesimal vertical thickness. We similarly assume that the corona is a pair of spheres uni-

form inside, each of radius R_h, and centered a distance h from the disc midplane (when $h = 0$, the two collapse into a single sphere). This simplified description should be an adequate qualitative stand-in for any coronal geometry which is unitary (i.e. not broken into many pieces), axisymmetric, and reflection symmetric about the disc plane. Both C and D may then be written in terms of R_s/R_h and h/R_h. We computed C taking into account electron scattering of the reflected radiation in the corona and assuming that the reflection emissivity is $\propto (r^2 + \hbar^2)^{-3/2}$ (where $\hbar$ is the averaged height of the corona above the disc plane) and its angular distribution is $\propto \cos\theta$. In computations of D, we assumed that the disc surface brightness is $\propto r^{-3}$ and its intensity distribution is isotropic, i.e., $p(\theta) = 2\cos\theta$. Contour plots of the coefficients C and D are presented in Figure 2. From C and D we can determine both R_s/R_h and h/R_h.

With these relationships and assumptions, we arrive at the derived quantities set out in Table 2. Although they are based on approximate expressions (and setting $4\pi da/d\Omega = 0.3$, along with $p = f_{\rm col}^2 f_{\rm GR}^2/f_m = 1$), we will show in the following section that they are confirmed with only small quantitative corrections by detailed calculations.

We can determine from Figure 2 that in the hard state $h/R_h \simeq 0.2$. This corresponds to an almost spherical corona. The cold disc penetrates only a short way into the corona (see Gierliński et al. 1997a and Dove et al. 1997 for a similar conclusion). If the disc were filled, relatively small C could be achieved for large τ due to electron scattering of the reflection component, but it would be difficult to get D small. The same argument also holds if the corona is larger than the disc (it would be easy to find geometries in which C is small, but then it becomes more difficult for D to also be small). In the soft state, $h/R_h \approx 0.5$, so that the corona is slightly elongated along the axis of the system (an outflow?). Now, the corona covers a significant fraction of the inner disc ($R_s/R_h \approx 0.6$).

There is, of course, some uncertainty in determining C and D from observations. C is usually known with $\sim 25\%$ accuracy. This translates into similar uncertainty in R_s/R_h,

and $\sim 50\%$ uncertainty in h/R_h. Estimations of D that are uncertain within a factor of 2 (mostly due to the strong dependence on the spectral index α) translate to $\sim 30\%$ and $\sim 15\%$ uncertainty in R_s/R_h for the SS and HS, respectively, while h/R_h is almost unaffected.

3 DETAILED CALCULATIONS

To verify these approximate arguments and refine our estimates of the inferred system parameters, we have computed exact numerical equilibria for a variety of parameters. We solved energy balance and electron-positron pair balance equations coupled with the radiative transfer. This was done using the code described in Poutanen & Svensson (1996). We assumed that the corona is spherical and centered on the black hole (i.e. $h = 0$), based on the fact that in both states the derived value of h/R_h is significantly smaller than 1.

We divided these calculations into two sets, one designed to mimic the hard state, the other the soft. All but one of the system parameters needed to define an equilibrium are given by the analytic estimates of the previous section. The one exception is τ_p, the net lepton optical depth. Although the total optical depth τ_T is reasonably well determined by observations, τ_p is not, because there is no easy way to tell from observations what portion of the Compton opacity is due to $e^{\pm}$ pairs. In terms of the ratio $z \equiv n_+/n_p$, $\tau_T = \tau_p(2z + 1)$. The one free parameter of the calculations is therefore τ_p.

In the hard state models, we fixed $l_h = 20$, $T_s = 0.13$ keV, $L_s^{\text{intr}}/L_h = 0.1$, and $R_s/R_h = 0.9$, and let $\tau_p = 0$, 1.0, and 2.0 (models HS1, HS2, HS3, respectively). Calculations gave $(\tau_T, \Theta, z) = (0.87, 0.39, \infty)$ for model HS1, $(1.12, 0.31, 0.06)$ for HS2, and $(2.001, 0.16, 0.0002)$ for HS3. Selected predicted spectra are compared with observations in Figure 3. When $\tau_p \ll 1$, pairs dominate, and $\Theta \simeq 0.4$; $\tau_p \gtrsim 1$ leads to $z \ll 1$, and the greater optical depth depresses the electron temperature. The best agreement with the observed spectrum (and the quality of this agreement is actually quite good) is found with $\tau_T \simeq \tau_p \simeq 2$, *i.e.*, a state in which the pair contribution is negligible (assuming that pairs are thermal). Thus, the approximate parameters of Table 2 come very close both to a truly self-consistent equilibrium, and to producing an output spectrum like the one seen.

In the soft state models we fixed $l_h = 15$, $T_s = 0.4$ keV, $L_s^{\text{intr}}/L_h = 3$, and $R_s/R_h = 0.65$, and let $\tau_p = 0$, 0.1, and 0.3 (models SS1, SS2, SS3, respectively). We find the following results: $(\tau_T, \Theta, z) = (0.24, 0.37, \infty)$ for model SS1, $(0.25, 0.37, 0.75)$ for SS2, and $(0.32, 0.31, 0.03)$ for SS3.

In many respects, the soft state is quite similar to the hard state; it differs primarily in having roughly an order of magnitude smaller optical depth, and in the much greater importance of intrinsically generated soft photons. These changes do not alter very much the critical τ_p below which pairs dominate: it is still a few tenths. However, in contrast to the hard state, the best agreement with observations (and this fit is again quite satisfactory) is found with $z \gtrsim 1$. Again we see that the analytic arguments are reasonably good guides to the results of more exact calculation.
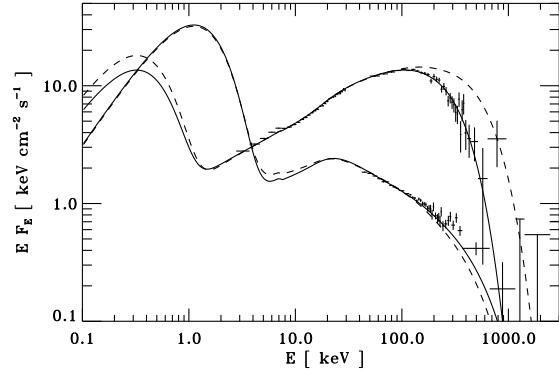

Figure 2. Theoretical spectra predicted by the calculations described in § 3. In both spectral states, the absolute normalization of the luminosity is arbitrary. The solid curve for the hard state corresponds to model HS3, and the dashed curve to model HS2 (inclination of the disc is assumed to be 30°). The solid curve for the soft state corresponds to model SS2, and the dashed curve to model SS3. The discrepancies between predictions and observations, particularly at the high energy end, for HS2 and SS3 show that there cannot be too many pairs in the hard state, or too few in the low state. The hard state data are from Gierliński et al. (1997a) and the soft state data are publically available from the HEASARC.

4 DISCUSSION

These inferences allow several strong conclusions to be made. Most importantly, the fact that such a self-consistent picture may be drawn gives additional support to the basic picture of thermal Comptonization for the origin of the hard X-rays. This suggestion was part of the original proposal of Shapiro et al. (1976), who suggested that in the hard state, the inner portion of the accretion disc puffs up into a hot Comptonizing corona. Their picture of the geometry is also confirmed. In addition, we now see that in the soft state the disc extends inward almost as far as it can, while the corona surrounds it out to several gravitational radii.

We are also now able to see that the disc receives only a minority of the dissipation in the hard state, but is the site of most of the heat release in the soft state. This conclusion is especially robust, for it depends primarily on the single ratio $L_h^{\text{obs}}/L_s^{\text{obs}}$. If we have overestimated L_s^{obs} in the hard state, the fraction of the dissipation taking place in the disc becomes even smaller.

The radius of the disc's inner edge shrinks by roughly a factor of 5 between the hard state and the soft state. This ratio is somewhat sensitive to several uncertainties. First, $R_s \propto [L_s^{\text{obs}}]^{1/2}$, and second, R_s in the soft state can be affected by uncertainty in the scaling factors $p(\theta)$, f_{col}, f_{GR}, and f_m. In terms of gravitational radii $r_g = GM/c^2$, $R_s \simeq 40 r_g M_{10}^{-1}$ in the hard state, and $\simeq 8 r_g M_{10}^{-1}$ in the soft state. Here M_{10} is the mass of the black hole scaled to $10 M_\odot$, the best estimate of Herrero et al. (1995).

Estimates of R_s, combined with the intrinsic luminosity of the disc, also permit us to place strong bounds on the mass accretion rate through the disc, $\dot{M}_d$. Almost independent of

the spin of the black hole, mass passing through a thin disc extending outward from the $\simeq 40r_g$ inferred for the hard state has a net binding energy $\simeq 0.02$ of its rest mass. The intrinsic disc luminosity, at least, must be drawn from this store of energy; $\dot{M}_d$ in the hard state must then be at least $0.4 \times 10^{-8} M_\odot$ yr^{-1} (this estimate is sensitive to uncertainty in L_s^{obs}; it scales roughly $\propto \left[L_s^{\mathrm{obs}}\right]^{3/2}$). The greatest possible $\dot{M}_d$ would be required if all the energy for coronal heating is taken from matter accreting through the disc (that is, inside R_s, the specific angular momentum of the matter changes, but not its specific energy). That upper bound is $\dot{M}_d \simeq 4 \times 10^{-8} M_\odot$ yr^{-1}. In the soft state, the efficiency of the disc varies from $\simeq 0.05$ (zero spin) to $\simeq 0.1$ (maximum rotation). Similar reasoning then gives a lower bound of $0.7 - 1.4 \times 10^{-8} M_\odot$ yr^{-1} and an upper bound only about 20% greater (because nearly all the luminosity in the soft state is radiated by the disc). If $\dot{M}_d$ in the hard state is near the lower bound, the efficiency of the inner corona in the hard state must be $\simeq 0.2$ in order to explain the total luminosity. If so, the black hole would have to be rotating relatively rapidly.

It is also of interest to compare $\dot{M}_d$ to the accretion rate which would produce an Eddington luminosity if radiation were created at the efficiency of a maximal Kerr black hole—$6 \times 10^{-8} M_{10} M_\odot$ yr^{-1}. In those units, the estimates of the previous paragraph give normalized accretion rates $\dot{m} = 0.07$ (or possibly as high as $\dot{m} = 0.7$) in the hard state, and $\simeq 0.1 - 0.2$ in the soft state.

Meanwhile, the corona shrinks in radial scale by only half as much as the disc when Cyg X-1 moves from the hard state to the soft. In the latter state, it covers a sizable portion of the inner disc. Despite the sharp change in size and luminosity, the compactness of the corona changes by no more than a factor of a few (incorporating the uncertainty in R_s) as a result of the hard-soft transition. However, its optical depth drops by an order of magnitude. Although there are few $e^\pm$ pairs in the equilibrium characterizing the hard state, they can be comparable in number to the net electrons in the soft state. This fact also means that the fall in τ_p from the hard state to the soft is even greater than the fall in τ_T.

We close by noting that in the hard state there must be a hole in the central region of the thermal disc which is much bigger than the radius of the innermost stable orbit. The origin of this hole is a question of prime importance. One possibility arises from the fact that the disc becomes dominated by radiation pressure inside $\simeq 35(\dot{m}/0.1)^{2/3}$ gravitational radii. As shown by Shakura & Sunyaev (1976), in the strict α-model, radiation pressure-dominated discs are thermally unstable. It is interesting that the inner radius of the disc in the hard state corresponds quite closely to this possible point of instability. We are then left with the question of how a thin disc is able to persist in to much smaller radius in the soft state, when $\dot{m}$ is still ~ 0.1. Another possibility is that the inner disc in the hard state is advection-dominated, while in the soft state the accretion rate is just a bit too high for that to happen (Narayan & Yi 1995). While the creation of an advection-dominated region may be a nonlinear end-state of the thermal instability, so that this model provides an attractive explanation for the hard state, it also leaves open how the thin disc survives thermal instability in the soft state.

REFERENCES

Bałucińska M., Hasinger G., 1991, A&A, 241, 439
Bałucińska-Church M., Belloni T., Church M. J., Hasinger G., 1995, A&A, 302, L5
Belloni T., Méndez M., van der Klis M., Hasinger G., Lewin W. H. G., van Paradijs J., 1996, ApJ, 472, L107
Cui W., Heindl W. A., Rothschild R. E., Zhang S. N., Jahoda K., Focke W., 1996, ApJ, 474, L57
Dotani T., Negoro H., Mitsuda K., Inoue H., Nagase F., 1996, IAU Circ. 6415
Dove J., Wilms J., Maisack M., Begelman M. C., 1997, ApJ, in press (astro-ph/9705130)
Ebisawa K., Ueda Y., Inoue H., Tanaka Y., White N. E., 1996, ApJ, 467, 419
Gierliński M., Zdziarski A. A., Done C., Johnson W. N., Ebisawa K., Ueda Y., Haardt F., Phlips B. F., 1997a, MNRAS, 288, 958
Gierliński M., Zdziarski A. A., Dotani T., Ebisawa K., Jahoda K., Johnson W. N. 1997b, in Dermer C. D., Kurfess J. D., eds, Proc. 4th Compton Symposium. AIP, in press (astro-ph/9707213)
Grove J. E. et al., 1997, in Winkler C., Courvousier T. J.-L., Durouchoux Ph., eds, Proc. 2nd INTEGRAL Workshop, ESA SP-382, The Transparent Universe. ESA, p. 197
Haardt F., Maraschi L., Ghisellini G., 1994, ApJ, 432, L95
Herrero A., Kudritzki R. P., Gabler R., Vilchez J. M., Gabler A., 1995, A&A, 297, 556
Narayan R., Yi I., 1995, ApJ, 452, 710
Mitsuda K. et al., 1984, PASJ, 36, 741
Phlips B. F., Jung G. V., Leising M. D. et al., 1996, ApJ, 465, 907
Pietrini P., Krolik J. H., 1995, ApJ, 447, 526
Poutanen J., Svensson R., 1996, ApJ, 470, 249
Shakura N. I., Sunyaev R. A., 1976, MNRAS, 175, 613
Shapiro S. L., Lightman A. P., Eardley D. N., 1976, ApJ, 204, 187
Shimura T., Takahara F., 1995, ApJ 445, 780
Stern B. E., Poutanen J., Svensson R., Sikora M., Begelman M. C., 1995, ApJ, 449, L13
Tanaka Y., Levin W. H. G., 1995, in Levin W. H. G., van Paradijs J., van den Heuvel, E. P. J., eds, Cambridge Astrophysics Series, Vol. 26, X-ray Binaries. Cambridge University Press, Cambridge, p. 126
Zdziarski A. A., Johnson W. N., Poutanen J., Magdziarz P., Gierliński M., 1997, in Winkler C., Courvousier T. J.-L., Durouchoux Ph., eds, Proc. 2nd INTEGRAL Workshop, ESA SP-382, The Transparent Universe. ESA, p. 373
Zhang S. N., Cui W., Chen W., 1997a, ApJ, 482, L155
Zhang S. N., Cui W., Harmon B. A., Paciesas W. S., Remillard R. E., van Paradijs J., 1997b, ApJ, 477, L95